Zagazig University Medical Journal
www.zumj.journals.ekb.eg
https://dx.doi.org/10.21608/zumj.2021.97027.2352 Volume 29, Issue 2, March 2023, Page (566-582)

Manuscript ID ZUMJ-2109-2352 (R1)
DOI 10.21608/zumj.2021.97027.2352

ORIGINAL ARTICLE

HISTOLOGICAL AND IMMUNOHISTOCHEMICAL STUDY ON THE EFFECT OF PRENATAL ADMINISTRATION OF DICLOFENAC SODIUM ON MATERNAL AND NEONATAL ORGANS IN ALBINO RAT

Hanan E.L. Mokhtar, Nadia Alabassery, Rasha Mohammad Sabry Hussein
Human anatomy and embryology, Faculty of Medicine, Zagazig University, Egypt.

Corresponding author:
Name: Hanan E.L. Mokhtar
Email address::
HAMokhtar@medicine.zu.edu.eg;
lotfyann@gmail.com
Phone: 01119532265

Submit Date	2021-09-21
Revise Date	2021-10-03
Accept Date	2021-10-09

ABSTRACT

Background: Diclofenac sodium (DS) can induce developmental abnormalities in embryos if consumed during pregnancy.

Objective: To assess the effect of prenatal administration of therapeutic dose of DS during the critical period of organogenesis on development of different neonatal organs of albino rats and on maternal organs, as well as to spotlight on the immunohistochemical reactions that may explain the possible impacts of DS**.**

Material and Methods: After mating, 18 pregnant rats were allocated into three groups. Group (I): received balanced diet, Group (II): received intraperitoneal injection (IP) of 1mL/kg/day of distilled water, Group (III): received IP of 1.5mg/Kg.bw/day of DS dissolved in distilled water from 7th - 14th days of gestation. The mothers (6/group) and their newborns (10/group) were anaesthetized following labor. The placentae and livers from mothers and hearts, livers, and lungs from their neonates were examined after preparation using light microscopy, immunohistochemical, morphometric studies and statistical analysis.

Results: Histologically, in all DS-treated groups, there was degenerative histopathological changes in the organs of both pregnant albino rats and their neonates. Morphometric and statistical analysis showed highly significant increase in the area percentages of positive TNF-α and iNOS immunoreactions in all DS-treated groups as compared to their control groups. Moreover, the most affected organ in mothers was the placenta while, the lung tissues in neonates.

Conclusion: The current investigation found that giving therapeutic doses of DS during the period of organogenesis caused significant histopathological alterations in both maternal and neonatal organs enhanced by upregulation of proinflammatory markers linked to oxidative stress.

Key words: Diclofenac sodium, Maternal and Neonates, albino rats, TNF-α, iNOS.

INTRODUCTION

Diclofenac sodium (DS) belongs to the chemical group of non-steroidal anti-inflammatory drugs (NSAIDs. It is one of most currently used medications of the NSAIDs group for the treatment of varieties of common chronic and acute inflammatory conditions in the obstetrics and gynecologic areas and clinics. It is also widely utilized by women in different periods as post-puberty for the management of pain of menorrhagia and dysmenorrhea and also during pregnancy and lactation for treatment of rheumatic disorders **(1-3).**

Utilizing NSAIDs during early pregnancy may be attributed to unawareness of pregnancy or a disregard for self-medication drug compositions. This may have adverse side effects and many negative alarming impacts on the mother and on development of fetal organs **(4-6).** The use of NSAID during pregnancy has been mentioned to cause difficult births or to increase the hazard of miscarriage in some women **(7, 8).**

Despite the fact that diclofenac's toxicity and teratogenicity have been recorded, inconsistent data has been published. Fetuses born following diclofenac treatment, displayed intrauterine growth

retardation, different skeletal, visceral and morphological anomalies, **(9, 10)** or associated with oligohydramnios (low amniotic fluid production) **(11),** cardiac septal defects **(12)**, premature closure of the fetal ductus arteriosus (DA) **(13),** pulmonary hypertension, severe respiratory distress **(14, 15),** morphological fetal renal abnormalities and neonatal renal failure(16), abnormal development of caudal neural tube and hind limb bud **(17)** and impairment development of peripheral nervous system **(18)**. Furthermore, in comparison to other NSAIDs, long-term use of Diclofenac treatment can cause liver damage and hepatotoxicity in both adult animals and human, and the severity of the injury is dependent on the length of exposure and dosage **(19, 20).**

Diclofenac displays its influence through the suppression of various events as cyclooxygenases (COX) enzyme activity (COX 1 and COX 2), and thus inhibits the transfer of arachidonic acid to a number of prostaglandin (PG) derivatives which are responsible for pain felling, inflammation, edema, and platelet aggregation **(2, 21).**

The impact of prostaglandin production inhibitors on development of fetal organs are not fully realized **(22, 23).** The studies dealing with the histological study of diclofenac toxicity on the developmental organs, were investigated on fetal and newly born Kidneys **(24, 25)**, on newborn testis **(26)**, on newborn hippocampus **(23)**, on cerebellum **(27).** on ovary and uterine horn **(28)** and on maternal and fetal livers **(29).**

To our knowledge, there no published works dealing with histopathology of different organs of both mothers and their offspring maternally treated with DS.

The aim of the present study is to assess the prenatal effect of administration of therapeutic dose of diclofenac sodium during critical period of organogenesis on architecture of different developmental organs of neonatal albino rats and on the maternal organs as well with spotlight on the immunohistochemical reactions that may explain its possible impacts. The effect was evaluated by histological, Immunohistochemical, morphometric studies and statistical analysis**.**

MATERIAL AND METHODS

Chemical: The drug chosen in the present study was diclofenac sodium (DS) (Declophen; pharco pharmaceutical company, Egypt). The selected dose of DS was 1.5 mg/kg body weight (bw) by intraperitoneal injection (IP) according to previous investigators **(25).** This diclofenac dose generated in rats, is nearly within the human therapeutic dose and it matches to the No Observed Adverse Effect Level (NOAEL) for fetal and maternal toxicity. A low effective dose for oral pain treatment in humans is 0.4 mg/kg/bw/6 hours (equivalent to 1.2 mg/kg/bw/day) **(30).**

Animals:

In this study, 18 healthy non pregnant adult female Wistar albino rats and 9 adult male albino rats (150-250 gm) were used for mating. The animals were gained from scientific medical research center (ZSMRC) at the Faculty of Medicine, Zagazig University. The experiment has been revised and accepted by Institutional Animal Care and Use Committee Zagazig University (ZU-IACUC) **(***approval number: **ZU-IACUC/3/F/109/2021***).**

For one week prior to the study, all animals were housed and kept in good hygienic circumstances under a 12/12-hour light/dark cycle and fed a balanced meal and tap water ad libitum. The rats were permitted to mate in individual plastic cages (females with males 2:1 respectively). When female rats' vaginal smears contained sperm or seminal plug after mating with males, it was considered the zero day of pregnancy. The Pregnant rats were equally allocated into three groups (6 rats /each group).

Group (I): Control group: 6 pregnant rats did not receive any treatment but fed only distilled water and balanced diet until the end of experiment.

Group (II): vehicle control group: 6 pregnant rats were given daily IP of 1 mL/kg of distilled water from 7^{th} -14^{th} days of gestation.

Group (III): DS-treated group: 6 pregnant rats were received daily IP of 1.5 mg/Kg bw of diclofenac sodium (DS) dissolved in distilled water from 7^{th} -14^{th} days of gestation**.**

At the end of experiments, after labor, the mothers (6/ each group) and their neonates at 1^{st} postnatal day (PD1) (10/each group) (19-25 g) were anesthetized by thiopental sodium (50 mg/kg bw) by IP **(31).** For neonates, they were fixed in formalin (10% neutrally buffered) for three days. To permit quick and complete penetration of the fixative to their internal organs, their skin was incised in various thoracic and abdominal places in addition to, 0.5 cm. of fixative was injected in their peritoneal cavities. The body was split longitudinally into two halves after the first 24 hours of fixation, returned to the fixative to finish fixation, and then rinsed under running water for 10-24 hours. However, for mothers, their abdomen was opened after dissection, the livers and placentae were quickly removed and were fixed in 10% neutral buffered formalin. The specimens were dissected out carefully, rinsed in phosphate buffer saline, prepared and examined by light microscopy, immunohistochemical and morphometric studies.

I-Histological examination:

A-Preparation for Light microscopy:

After collection and fixation of the samples, they were dehydrated in ascending grades of alcohol (50 % , 70 %, 90 %, and 95 %) then in absolute alcohol (100 %) for two changes (1 hour each) and processed to be implanted in paraffin according to previous investigators **(32).** Specimens slide sections of 4-5

µm were stained with Hematoxylin and Eosin. The histopathological examination and photography were established using light microscope (Leica DM500 with Leica ICC50 W" digital Camera) at the Image analysis unit of human anatomy and embryology department, Faculty of medicine, Zagazig University.

B-Preparation for Immunohistochemical (IHC) study:

Immunostaining was carried out by dewaxing of the paraffin sections (4 µm thickness), in fresh xylene for 20 minutes and transferred into descending grades of ethanol. The endogenous peroxidase activity was blocked by dealing with 10 % H2O2 for 15 minutes at room temperature. For one hour, the sections were incubated with the primary antibody against Tumor Necrosis Factor-alpha (TNF-α), used as a marker for proinflammatory cytokines (anti-TNF-α, a mouse monoclonal antibody; Dako, California, USA, Carpinteria; at a dilution of 1:50). In the same way, the sections were incubated with primary antibody against Inducible Nitric Oxide Synthase Enzyme (iNOS) as an oxidative stress marker (anti-iNOS, rabbit anti-rats polyclonal antibody, M-19/Sc 650, at 1:100 dilution, Santa Cruz Biotechnology, Santa Cruz, CA, USA). By using the streptavidin-biotin-peroxidase technique, the sections were incubated (20 min) with a secondary biotinylated antibody after rinsing with Phosphate-buffered saline (PBS). The secondary antibody binding was detected after incubation in 3,3-diaminobenzoic acid (DAB) as a chromogen for 20 min. The sections were washed with PBS before each step. The sections were then counter-stained using Mayer's hematoxylin. By omitting the primary antibody, the negative control sections were prepared. To confirm the success of the technique for all stains, the positive control slides were used. All slides were inspected by light microscopy and the cellular site of reactions were demonstrated in the cellular cytoplasm for the two markers. The presence of brown and yellow brown staining in TNF-α and iNOS immunostaining respectively**,** was documented as positive immunoexpression while the absence of staining was identified as a negative immunoreaction. All previous techniques for TNF-α and for iNOS immunostaining were done similar to the procedures of previous investigations **(24)** and **(33)** respectively. The immunostained slides were examined and photographed using Leica light microscope at Image analysis unit of human anatomy and embryology department, Faculty of medicine, Zagazig University**.**

II-Morphometric analysis:

The area percentages (%) of positive TNF-α and for iNOS immunostaining was morphometrically assessed in the stained sections at ×100 and ×400 magnifications using image analyzer (public domain image-processing software), "Image J" 1.49v/Java 1.6.0_244" (National Institutes of Health, USA). Firstly, the image analyzer was automatically adjusted to transform the image analyzer's measuring units (pixels) into real micrometer units. Ten non-overlapping fields were chosen at random from five slide slices from each specimen/group. The results were recorded as mean± standard deviation (SD) and compared to the control group by statistical analysis.

III-Statistical analysis:

Since the statistics had a normal distribution (parametric), the quantitative variables were provided in the form of mean ± standard deviation (SD). The GraphPad Prism® software programme, version 7, was used for statistical analysis (GraphPad Prism 7 Software Inc., San Diego, CA, USA). The independent T-test was used to discover significant differences between the control and treatment groups. When the P-value was <0.05, the values were judged statistically significant (*), and when the P-value was ≤0.0001, they were regarded highly significant (***).

RESULTS

I-Morphological assessment:

No aborted fetuses or dead rats or gross anomalies of organs were observed in the DS-treated group.

II- Histological examination using hematoxylin and eosin staining:

Histological examination of the sections of groups I and II revealed no difference. Therefore, results of group I were represented as the control group.

A-Maternal organs:

1-Placenta at term: (Figure 1. a-j):

Section of full-term maternal control placenta (group I) revealed that it was composed of three zones named; the decidua basalis, basal zone and the labyrinth zone. The labyrinth zone included the chief part of the placenta **(Fig. 1a).** The basal zone exhibited three differentiated cell types named; glycogenic, trophoblastic giant and numerous numbers of spongiotrophoblast cells **(Fig. 1b)**. The trophoblastic giant cells lied just above the decidua basalis and had characteristic shapes with large nuclei and prominent dense nucleoli **(Fig. 1c).** Many glycogenic cells were seen aggregated in islands while, small dense basophilic spongiotrophoblast cells were dispersed within the basal zone **(Fig. 1d)**. However, the labyrinth zone contained also three components named; maternal sinusoids, fetal capillaries and trophoblastic cells in between. The fetal capillaries were lined by double endothelial layers containing erythroblast however, the maternal sinusoids contained erythrocytes. The trophoblastic cells showed small rounded densely stained nuclei **(Fig. 1e)**.

In the DS-treated placenta (group III), as regard to the basal zone, there was marked reduction of islands of glycogenic cells with the development of enormous coalescing cysts (containing eosinophilic cellular debris) instead. Single island of glycogenic cells was seen migrating in labyrinth zone instead of its location in basal zone. The normal

spongiotrophoblasts cells were decreased in number with necrosis and pyknosis of some of them. The trophoblastic giant cells were markedly decreased in number and size and appeared with shrinked or disintegrated nuclei**.** In addition, there was apparent dilatation and congestion of blood vessels within the basal zone **(Figs. 1f-1g)**. In the labyrinth zone, extensive hemorrhage with rupture of the nearby blood vessels were well observed **(Fig. 1h)**. Moreover, in the labyrinth zone, marked vasodilatation and congestion of both maternal sinusoids and fetal capillaries were also demonstrated. Many numbers of trophoblastic cells were obviously degenerated if compared with the control group within the labyrinth zone **(Figs. 1i, 1j).**

2- Maternal liver (Figure 2. a-e):

Light microscopic examination of the maternal control liver (group I) indicated its normal structure. Well-formed hepatic cords were seen radiating from a thin walled central vein. The hepatic cords exhibited well-developed polygonal-shaped hepatocytes. The hepatocytes contained central rounded vesicular nuclei with small nucleoli inside acidophilic cytoplasm. Vascular spaces called blood sinusoids between the hepatic cords were seen lined by flat endothelial cells **(Fig. 2a)**. There was a small portal area with branches of typical portal vein, hepatic artery, and bile ductule lined by simple cuboidal epithelial cells. The portal area was surrounded by thin periportal connective tissue **(Fig. 2b)**.

The DS maternal treated group (III) revealed many signs of hepatic structure deteriorations. The blood sinusoids were moderately dilated and contained proliferated kupffer lining cells. The central veins and some sinusoids were seen dilated and congested with hyaline casts. **(Fig. 2c**). Most of hepatocytes appeared swollen and vacuolated. Some of them appeared with large nucleoli within vesicular nuclei and some were necrotic marked by pyknotic nuclei with condensed chromatin **(Fig. 2d)**. Moreover, the portal area was extensively enlarged and contained markedly dilated and congested thick-walled portal vein. Bile ductule proliferation was well seen and was bordered by dense connective tissue. The hepatic arteries with thickened wall were also demonstrated **(Fig. 2e)**.

B-Neonatal organs (1st postnatal day, PD1):

1- Neonatal liver: (Figure 3. a-f)

The hepatic parenchyma of the newly born rat control liver of group (I) displayed small sinusoidal spaces between the hepatic cords, drained into central vein which was lined by thin endothelium. The hepatocytes exhibited acidophilic cytoplasm with central vesicular nuclei. The hematopoietic (blood forming) cells were observed densely stained and aggregated in groups **(Fig. 3a).** In addition, the portal area contained portal vein, hepatic artery and bile ductules lined by simple cuboidal epithelium **(Fig. 3b).**

In the neonatal treated liver (group III), showed extensive destructive changes in the form of congestion and dilatation of the central vein**s**, extensive cytoplasmic vacuolations of hepatocytes and some hemorrhagic areas in between **(Fig. 3c).** In other areas, the central vein appeared dilated without congestion but with distorted epithelial lining. Moreover, necrosis of many hepatocytes was also observed **(Fig. 3d)**. The hematopoietic (blood forming) cells were increased in number and seen dispersed. Some of them appeared collected nearby the dilated sinusoid or present within the lumen of central vein. Many binucleated giant cells were also noticed **(Fig. 3e).** Marked dilatation of portal vein and proliferation of bile ductules with thickening of their walls were also observed in the portal area **(Fig. 3f).**

2- Neonatal lung: (Figure 4. a-f):

The control lung tissue of newly born albino rat (group I) showed normal structures in the form of; terminal bronchioles, dispersed air saccules and air spaces separated by relatively thick mesenchymal tissue of lung parenchyma. The air spaces showed secondary crests projecting from their walls to form saccules. The pulmonary vessels with thin walls were seen associated with terminal bronchioles and adjacent to air spaces **(Fig. 4a).** The terminal bronchioles were lined with respiratory epithelium. The mesenchymal tissue of lung parenchyma was composed of numerous cells possessing darkly stained nuclei **(Fig. 4b)**.

By comparing with the control group, the neonatal lung treated with DS (group III) showed shrinkage of lung tissue and the air spaces appeared markedly decreased in size. The pulmonary blood vessels nearby terminal bronchioles appeared markedly dilated and congested **(Fig. 4c).** Other degenerative changes to the treated lung tissues were in the form of; extensive cytoplasmic vacuolations in mesenchymal cells of lung parenchyma and within the epithelium of terminal bronchioles, detachment and disruption of epithelial lining of the terminal bronchioles, edema and hemorrhage in mesenchymal tissue and dispersed blood spots between the mesenchymal tissues **(Fig. 4d-4e).** The congested blood vessel next to bronchiole had also vacuolated cells in its wall as well **(Fig. 4f)**.

3- Neonatal heart: (Figure 5a-e)

The control sections of the ventricular wall of newly born rat heart (group I) showed bundles of longitudinal and transverse fibers of cardiac muscles. The longitudinal bundles were composed of elongated muscles fibers called cardiac myocytes or cardiomyocytes **(Fig.5a)**. The cardiomyocytes exhibited striated eosinophilic cytoplasm and slightly elongated central vesicular nuclei. Narrow connective tissue (CT) spaces between the cardiac muscle fibers showed few fibroblasts with flat nuclei and small blood capillaries **(Fig. 5b)**.

However, the DS-treated neonatal rat heart (group III) when contrasted with control group of the same age revealed massive degenerative changes. Between the cardiac muscle fibers, extensive areas of hemorrhage, extravasated hemorrhage and markedly dilated and congested blood capillaries were seen. Moreover, extensive cytoplasmic vacuolations with nuclear pyknosis of cardiomyocytes and extracellular edema in between were also clearly observed **(Figs. 5c-5e)**.

III- Immunohistochemical analysis:

1- TNF-α immunostaining for Maternal organs:(Figure 6a-d):

Sections of control groups (I) showed faint TNF-α reactions in the basal zone of placenta **(6a)** and in the cytoplasm of hepatocytes **(6b)**. However, the DS-treated groups (III) displayed wide areas of strong positive TNF-α immune reactions (as brown coloration) in the labyrinth and basal zones of placenta **(6c)** but moderate reaction in cytoplasm of hepatocytes **(6d)** as compared with placenta**.**

2- TNF-α immunostaining for Neonatal organs (Figure 7a-f):

Sections of neonatal control liver (7a), lung (7b) and heart (7c) of groups (I) showed negative TNF-α immune reactions. However, the DS-treated groups (III) showing apparent patches of positive TNF-α immune cytoplasmic reactions as (brown coloration) in liver (7d), lung (7e) and heart (7f) tissues.

3- iNOS immunostaining for maternal organs:(Figure 8a-d):

Sections of control groups (I) showed faint iNOS expression in the basal zone of placenta **(8a)** and negative reaction in the cytoplasm of hepatocytes **(8b)**. However, the DS-treated groups (III) displayed strong positive iNOS immune expression (as yellow brown coloration) in the labyrinth and basal zones of placenta **(8c)** and in cytoplasm of hepatocytes **(8d).**

4- iNOS immunostaining for neonatal organs (Figure 9a-f):

Sections of neonatal control liver (9a), lung (9b) of groups (I) showed negative iNOS immuno-expressions but faint in heart (9c). However, the DS-treated groups (III) showed strong positive iNOS immune cytoplasmic expressions (as yellow brown coloration) in liver (9d) and in lung (9e) tissues but mild positive expression appeared in heart tissue (9f) as compared with other treated organs.

IV- Morphometric and statistical analysis:

In all studied groups, the statistical results using independent T-test, showed highly significant increase in the mean values of area % of positive TNF-α and iNos immuno-reactions (**P**<0.0001) in the DS-treated groups (III) as compared to their control groups (I). Moreover, the most affected organ in mothers was the placenta (area % of TNF-α and iNOS immunostaining = 6.9 ± 0.60 and 14 ± 3.3 respectively), while in neonates was the lung (area % of TNF-α and iNOS immunostaining = 1.4 ± 0.34 and 16 ± 2.4 respectively) if they compared with area % of other treated organs (**Tables** 1 and 2) and (**Bar charts** 1-10 in figures 6-9).

Table 1. Statistical assessment of mean values of area percentages of positive TNF-α immuno-reaction among control and SD- treated groups using independent T-test.

Groups	control	DS-treated	t- value	P- value
Placenta	0.58 ± 0.015	6.9 ± 0.60	9.7	<0.0001***
Maternal liver	0.083 ± 0. 01	1.3 ± 0.10	11	<0.0001***
Neonatal liver	0.034 ± 0.027	0.74 ± 0.091	25	<0.0001***
Neonatal lung	0.060 ± 0.042	1.4 ± 0.34	13	<0.0001***
Neonatal heart	0.040 ± 0.0070	0.88 ± 0.055	50	<0.0001***

N=10 for each subgroup

***: Highly significant difference (P<0.0001) between control and DS treated group

Table 2. Statistical assessment of mean values of area percentages of positive iNOS immuno-reaction among control and SD- treated groups using independent T-test.

Groups	control	DS-treated	t- value	P-value
Placenta	1.1 ± 0.37	14 ± 3.3	13	<0.0001***
Maternal liver	0.046 ± 0.018	10 ± 3.6	9.5	<0.0001***
Neonatal liver	0.080 ± 0.047	13 ± 3.3	14	<0.0001***
Neonatal lung	0.094 ± 0.062	16 ± 2.4	22	<0.0001***
Neonatal heart	0.17 ± 0.048	1.9 ± 0.20	28	<0.0001***

N=10 for each subgroup

*** Highly significant difference (P<0.0001) between control and DS treated group

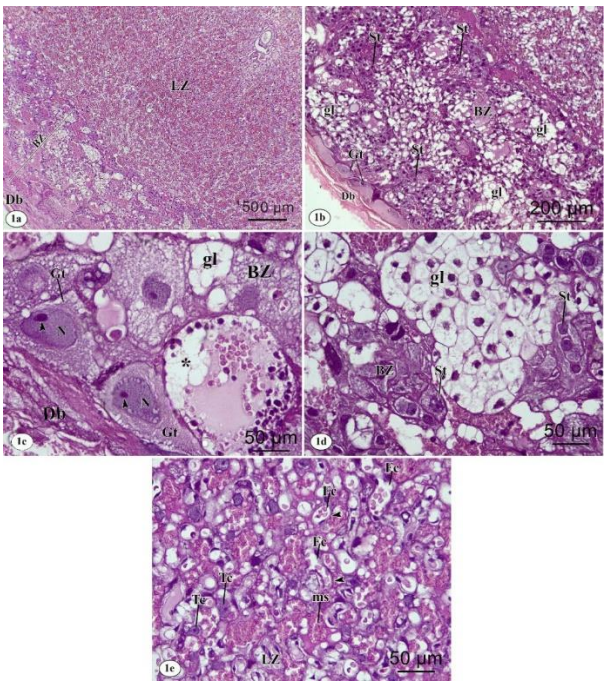

Fig. [1.a-e]: Photomicrographs of sections of full-term maternal placentae of control albino rats. **[a]:** showing three zones of placenta naming; decidua basalis (Db), basal zone (BZ) and labyrinth zone (LZ). **(H&E ×40) [b]:** showing the basal zone (BZ) containing glycogenic (gl), trophoblastic giant (Gt) and numerous numbers of spongiotrophoblasts (St) cells. **(H&E ×100) [c]:** The trophoblastic giant cells (Gt) lie above decidua basalis (Db) and exhibit large nuclei (N) and prominent dense nucleoli (arrowheads) within the basal zone (BZ). Notice the newly formed (gl) and newly developed glycogenic cells (*) are clearly seen. **[d]**: The glycogenic cells (gl) are aggregated in islands. Small spongiotrophoblasts (St) cells appear basophilic and dispersed. **[e]:** The LZ contains maternal sinusoids (ms), fetal capillaries (Fc) and trophoblastic cells (Tc) in between. Notice the fetal capillaries (Fc) are lined by double endothelial layers (arrowheads). The trophoblastic cells (Tc) have small rounded densely stained nuclei. **(H&E c-e ×400)**

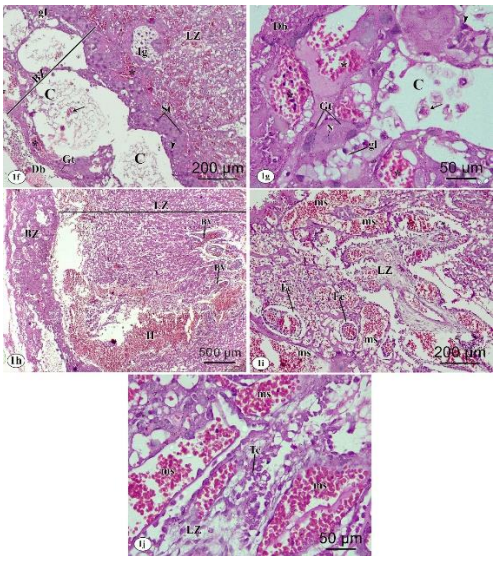

Fig. [1.f-j]: Photomicrographs of sections of full-term maternal placentae of DS-treated albino rats. **[f-g]:** showing marked reduction of islands of glycogenic cells (gl) in the basal zone (BZ). Enormous coalescing cysts (C) contain eosinophilic cellular debris (arrow) are seen in BZ. Single island of glycogenic cells (Ig) is seen migrating to LZ. The normal spongiotrophoblasts cells (St) are decreased in number and some of them appear small darkly stained (arrowhead). The trophoblastic giant cells (Gt) appear small with shrinked or disintegrated nuclei (N). Notice dilated and congested blood vessels (*) in BZ. Decidua basalis (Db) **(H&E f: ×100, g: ×400) [h]:** showing extensive hemorrhage (H) with nearby ruptured blood vessels (BV) are seen in LZ. **(H&E ×40) [i-j]:** showing vasodilatation with congestion of both maternal sinusoids (ms) and fetal capillaries (Fc). Many numbers of trophoblastic cells (Tc) appear degenerated in LZ**. (H&E i: ×100, j: ×400)**

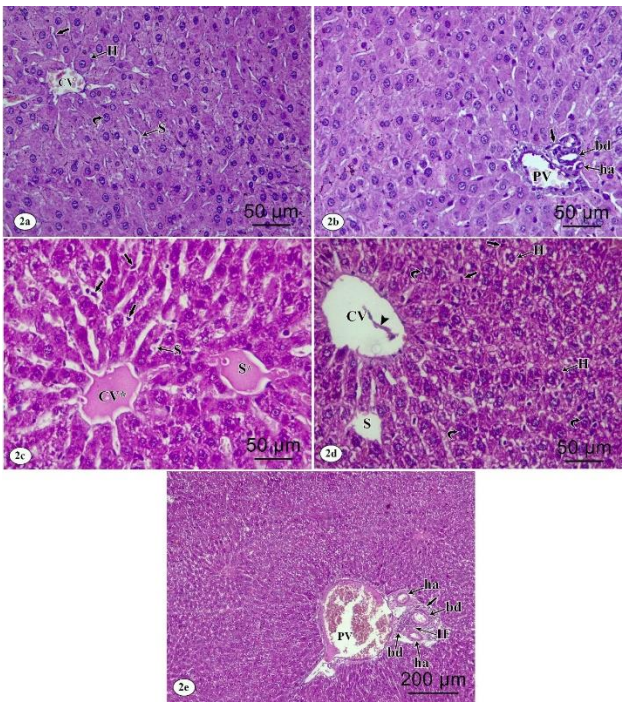

Fig. [2. a-e]: Photomicrographs of sections of maternal livers of control and SD-treated albino rats. **[a-b]:** sections of control maternal rat liver. **[a]:** showing polygonal-shaped hepatocytes (H) organized in cords irradiant from a central vein (CV). The hepatocytes (H) show central vesicular nuclei with small nucleoli (curved arrow). Narrow blood sinusoids (S) between the cords are lined by thin flat endothelial cells (Thick arrow) **(H&E × 400)**. **[b]:** showing portal vein (PV), hepatic artery (ha), bile ductule (bd) and all are surrounded by thin connective tissue (arrow) **(H&E × 400)**. **[c-e]:** Sections of maternal rat liver treated with DS. **[c]:** showing dilatation and congestion of central vein (CV*) and some sinusoid (S*) with hyaline casts. The dilated blood sinusoids (S) contain proliferated kupffer cells (arrows) **(H&E ×400)**. **[d]**: showing most of the hepatocytes (H) are swollen and vacuolated. Some hepatocytes appear with large nucleoli within vesicular nuclei (curved arrow) or with pyknotic nuclei (arrow). Notice dilated sinusoid (S) and central vein (CV) containing detached its epithelial lining are seen (arrowhead) (**H&E × 400)**. **[e]:** Portal vein (PV) has thick wall and markedly dilated, congested with blood cells. The bile ductules (bd) are dilated and proliferated and surrounded by thick connective tissue (arrow) with few cellular infiltrations (IF). Two hepatic arteries (ha) appear with thick wall **(H&E × 100)**.

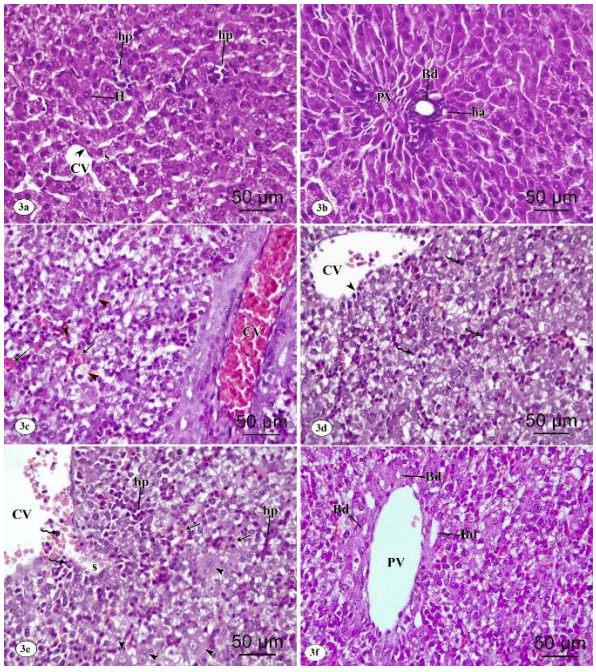

Fig. [3. a-f]: Photomicrographs of sections of neonatal livers of control and SD-treated PD1 albino rats. **[a-b]:** Sections of control rat liver. **[a]:** showing central vein (CV) with normal endothelial lining (arrowhead), sinusoids (S), hepatocytes (H) and hematopoietic cells (hp). **[b]:** showing portal vein (PV), hepatic artery (ha) and bile ductules (Bd). **[c-f]:** Sections of newly born rat liver treated with DS. **[c]:** showing dilated, congested central veins

(CV), extensive number of vacuolated hepatocytes (arrowheads) and areas of intercellular hemorrhage (arrow). **[d]:** showing dilated central vein (CV) with distorted epithelial lining (arrowhead) and necrotic hepatocytes (zigzag arrow). **[e]:** showing increased the number of hematopoietic cells (hp) forming blood (arrow). Notice some of them (zigzag arrows) are present adjacent the dilated sinusoid (s) or within the lumen of central vein (CV). Many binucleated giant cells (arrowheads) are seen**. [f]:** showing markedly dilated portal vein (PV)**.** The bile ductules (Bd) are seen upregulated. **(H&E × 400)**.

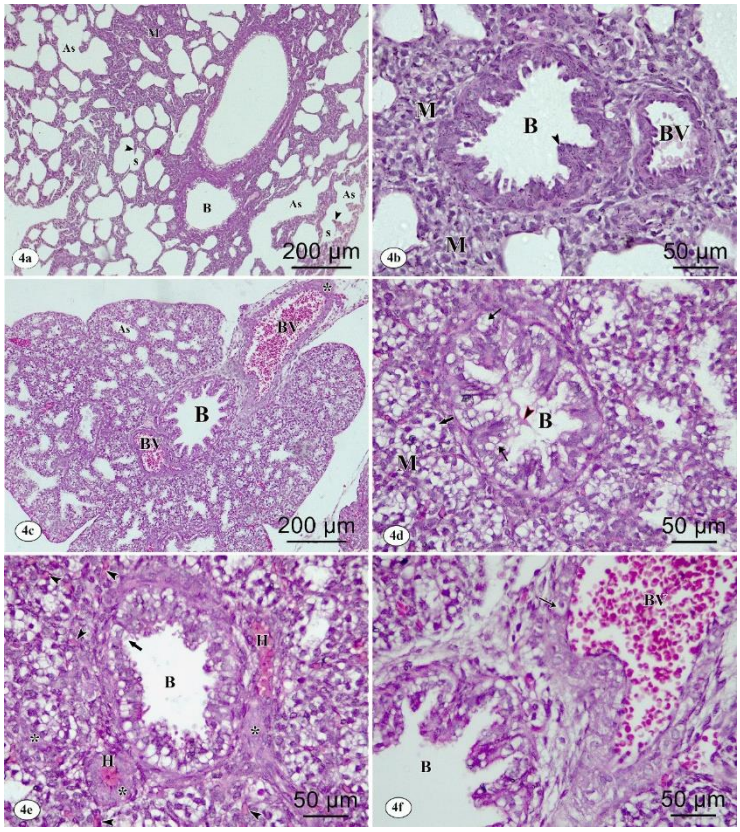

Fig. [4.a-f]: Photomicrographs of sections of neonatal lungs of control and SD-treated PD1 albino rats. **[a-b]:** Sections of control rat lung. **[a]:** showing terminal bronchioles (B), air spaces (As) and saccules (s). The air spaces (As) appear with secondary crests (arrowheads) projecting from their walls. Relatively thick mesenchymal tissue (M) of lung parenchyma is present in-between these structures. **(H&E ×100) [b]:** The terminal bronchioles (B) are lined with respiratory epithelium (arrowheads) with normal blood vessel (BV) is seen nearby it. The mesenchymal tissue (M) shows numerous cells possessing darkly stained nuclei. **(H&E ×400) [c-f]:** Sections of rat lung treated with DS. **[c]:** Air spaces (As) appear markedly decreased in size. Markedly dilated and congested pulmonary blood vessels (BV) adjacent to terminal bronchiole (B) are seen**. (H&E ×100) [d]:** showing extensive cellular vacuolations (thick arrows) of mesenchyme (M) and within the epithelium of terminal bronchioles (thin arrows). The epithelial lining of the terminal bronchiole (B) is seen detached (arrowhead). **(H&E ×400) [e]:** showing the terminal bronchiole (B) surrounded by hemorrhagic (H) and edematous (*) mesenchyme. Notice disrupted bronchiolar epithelium (arrows) and dispersed blood spots (arrowheads) between mesenchymal tissue. **(H&E ×400) [f]:** The congested blood vessel (BV) next to bronchiole (B) shows vacuolated cells (arrow) in its wall. **(H&E ×400)**

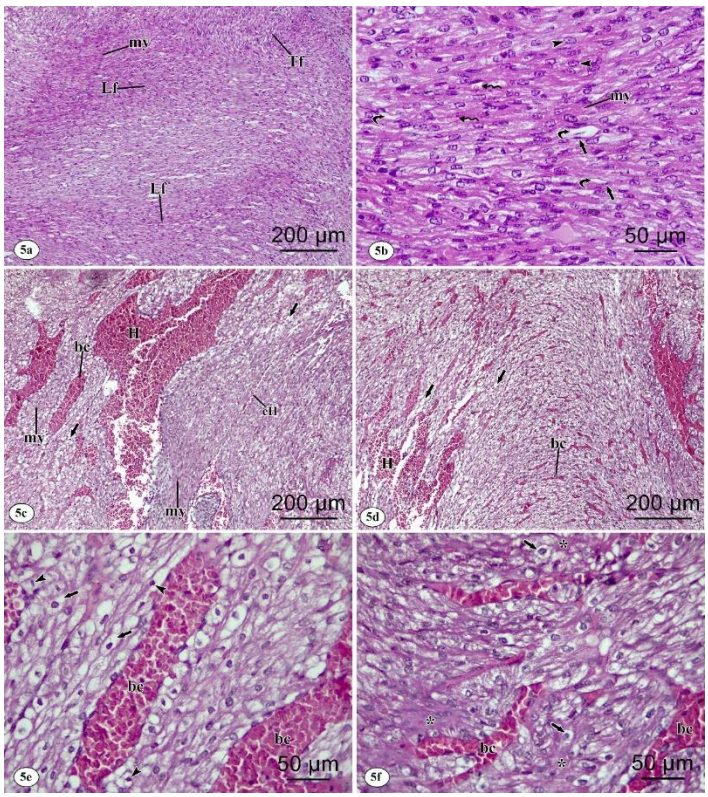

Fig. [5.a-f]: Photomicrographs of sections of neonatal hearts (ventricular wall) of control and SD-treated PD1 albino rats. **[a-b]:** Sections of control rat heart. **[a]:** showing bundles of longitudinal (Lf) and transverse (Tf) fibers of cardiac muscles (my). **(H&E ×100) [b]:** showing cardiomyocytes (my) containing striated eosinophilic cytoplasm and ovoid or slightly elongated central vesicular nuclei (arrowheads). Narrow CT spaces (curved arrow) between muscle fibers contain few fibroblasts with flat nuclei (arrows) and small blood capillaries (zigzag arrow). **(H&E ×400). [c-f]:** Sections of rat heart treated with DS showing extensive areas of hemorrhage (H), extravasated hemorrhage (eH), vasodilated and congested blood capillaries (bc) in between cardiomyocytes (my). Extensive vacuolations (arrows) and nuclear pyknosis (arrowheads) of cardiomyocytes with extracellular edema (*) between muscle fibers are also clearly observed. **(H&E c,d ×100 e,f ×400)**

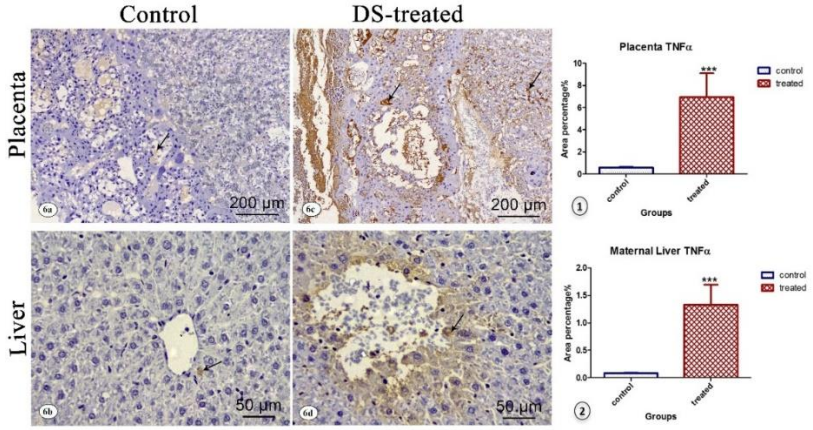

Fig. [6. a-d]: Photomicrographs of TNF-α immunostained sections of full-term maternal placentae and livers of control and SD-treated albino rats**. [a-b]:** sections of control groups showing faint TNF-α immune reaction in the basal zone of placenta **(a)** and in the cytoplasm of hepatocytes (arrow) **(b)**. However, **[c-d]**: sections of the DS treated groups showing strong brown positive TNF-α immune reactions (arrows) in the labyrinth and basal zones of placenta **(c)** and moderate reaction in cytoplasm of hepatocytes (arrow) **(d). [TNF-α IHC (placenta ×100) and (liver×400)]. Bar charts (1-2):** showing statistical assessment of the mean values of area % of TNF-α expression in placenta and maternal liver of control and treated groups as ***highly significant difference ($P < 0.0001$) as compared with the same control group by using independent T-test. The values are presented as mean ± SD.

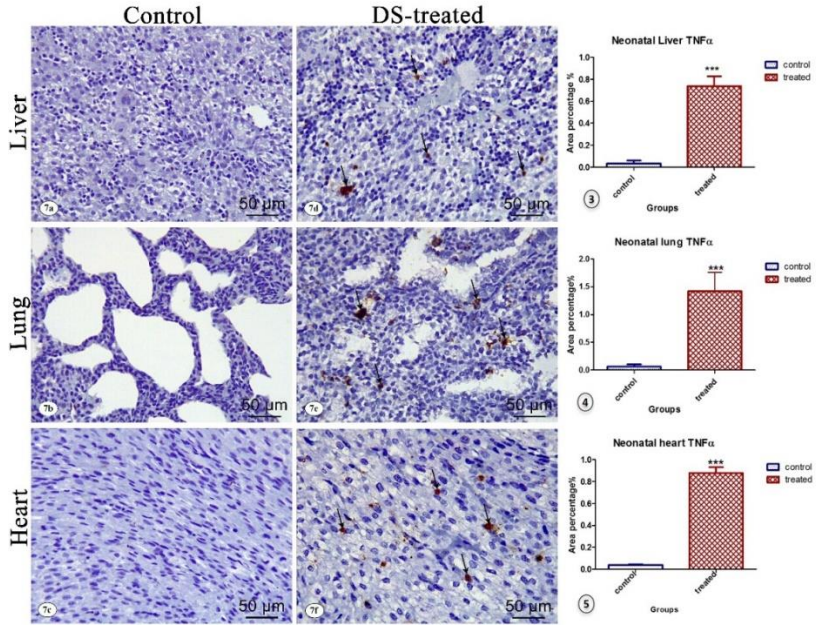

Fig. [7. a-f]: Photomicrographs of TNF-α immunostained sections of neonatal livers, lungs and hearts of control and SD-treated PD1 albino rats**. [a-c]:** Sections of control groups showing negative immune reactions in liver (a), lung (b) and heart (c) tissues. However, **[d-f]**: Sections of the DS treated groups showing apparent patches of brown positive TNF-α immune cytoplasmic reactions in liver (d), lung (e) and heart (f) tissues (arrows). **(TNF-α IHC ×400). Bar charts (3-5):** showing statistical assessment of the mean values of area % of TNF-α expression in neonatal liver, lung and heart of control and treated groups as ***highly significant difference (P<0.0001) as compared with the same control group by using independent T-test. The values are presented as mean ± SD.

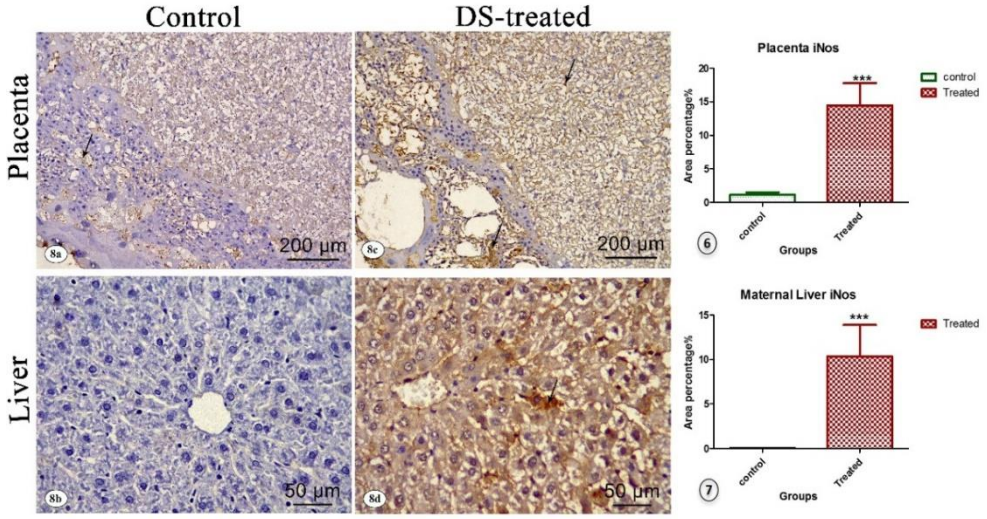

Fig. [8. a-d]: Photomicrographs of iNOS immunostained sections of full-term maternal placentae and livers of control and SD-treated albino rats**. [a-b]:** sections of control groups showing faint iNOS immune reaction (arrow) in the basal zone of placenta **(a)** and negative reaction in hepatocytes **(b)**. However, **[c-d]**: sections of the DS treated groups showing strong yellow brown positive iNOS immune reaction (arrows) in the labyrinth and basal zones of placenta **(c)** and in cytoplasm of hepatocytes **(d). [iNOS IHC (placenta ×100) and (liver×400)]. Bar charts (6,7):** showing statistical assessment of the mean values of area % of iNOS expression in maternal placenta and liver of control and SD-treated groups as ***highly significant difference (P < 0.0001) as compared with their control groups by using independent T-test. The values are presented as mean ± SD.

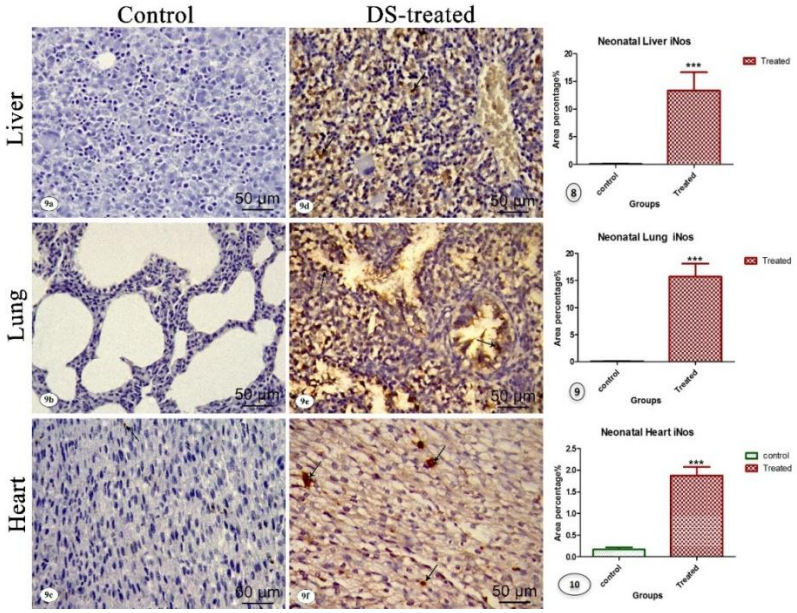

Fig. [9. a-f]: Photomicrographs of iNOS immunostained sections of neonatal livers, lungs and hearts of control and SD-treated PD1 albino rats**. [a-c]:** sections of control groups showing negative immune reactions in liver and lung but faint in heart tissue (arrow). However, **[d-f]**: sections of the DS-treated groups showing strong yellow brown positive iNOS immune cytoplasmic reactions in liver (d) and lung (e) tissues but mild positive reaction in heart (f) (arrows). **(iNOS IHC ×400). Bar charts (8-10):** showing statistical assessment of the mean values of area % of iNOS expression in neonatal liver, lung and heart of control and SD-treated groups as ***highly significant difference (P < 0.0001) as compared with their control groups by using independent T-test. The values are presented as mean ± SD.

DISCUSSION

As analgesics, anti-inflammatories, and antipyretics, NSAIDs are frequently used in the treatment of a wide range of medical problems **(23).** Diclofenac sodium (DS), which was employed in this study, is an NSAID derivative and one of the medicines routinely prescribed by obstetricians, gynecologists, and orthopedists. **(3)**. Despite the fact that the medical community is aware of the dangers of DS, most women are uninformed that NSAIDs are not recommended during the first and third trimesters of pregnancy. Furthermore, because many NSAIDs are accessible over the counter, the general public has a perception of safety. NSAIDs are commonly used to treat common illnesses in women, such as headaches, joint pain, and menstruation pain and so these patients often remain use NSAID in pregnancy **(34).** Furthermore, the United States Food and Medicine Administration (US.FDA) has categorized diclofenac as a pregnancy risk class C drug before 30 weeks of gestation and class D drug after 30 weeks and recommended that it should be used with caution during pregnancy**(35).** Consequently, DS was chosen as a pharmacological agent in the current study.

The main objective of this study was to investigate the prenatal impact of therapeutic dosage administration (1.5 mg/Kg bw) of DS on architecture of different developing organs of neonatal albino rats, as well as maternal organs throughout the critical period of gestation.

Unlike previous studies **(5, 36)** in which DS was given from the early gestational period until the end of pregnancy, we prefer to administer the drug during the middle week of the gestational period only and not until advanced gestational age. The most serious period of organogenesis in rats is from 6^{th} -15^{th} days of gestation for development of cardiovascular and midline organs. This period is corresponding to 3–6 weeks post fertilization in human embryos. The organs are tremendously susceptible to the influence of the toxic materials in these periods **(37)**.

The adverse effects of toxic doses of DS was assessed by many studies, so the chosen dose of diclofenac used in our study is nearly within the human therapeutic dose and it matches to the No Observed Adverse Effect Level (NOAEL) for maternal and fetal toxicity **(30).** Specifically, to report any possible teratogenic effects that may arise as a result of common drug abuse, NSAIDs are not recommended throughout the first and third trimesters, but their use is on the increasing.

In this work, we used a low dose of the drug (1.5 mg/Kg bw) to make in consideration the species differences, as suggested by **Yilmaz et al. (38)** who demonstrated considerable differences in pulmonary metabolic activity between humans and rats, owing to species and tissue dependent expression of drug metabolizing enzymes.

Poor palatability of the treated diet or water will result in a dose-related decrease in food or water consumption and will have an impact on the test drug intake **(39),** Therefore, In the current study we prefer the intraperitoneal injection as the route of drug administration.

NSAIDs may not be recognized as a safe analgesic or antipyretic treatment in the advanced 2nd trimester, according to the recent study **(40)**. After prenatal exposure to NSAIDs, fetal and neonatal

deleterious effects on the brain, kidney, lung, bone, gastrointestinal tract, and cardiovascular system have been observed **(4).** In addition, **Chan et al. (17)** revealed that DS had a direct teratogenic effect on rat embryos developed in vitro from gestational day 9.5 to11.5, even at low concentrations.

It is necessary to investigate the harmful effects of diclofenac on several mammalian cells in order to establish its mode of action, mechanisms, and severe toxic impacts, thereby aiding in the awareness against this developing contaminant **(41)**. To our knowledge, there was no published works dealing with histopathology of different organs of both mothers and their offspring maternally treated with DS.

The placenta not only serves as a link between two unique individual circulations (maternal and fetal) and promoting normal fetal development and growth, it also acts as a protective barrier for the fetus against xenobiotics in the maternal circulation**(42, 43).**

The placental barrier permeability to the drug, fetal gestational age are factors that influence deleterious consequences in pregnancy **(2).** To some extent, the placenta is selectively permeable. Diclofenac is thought to be the most toxic member of NSAIDs, can breach the placental barrier and pass from mother to fetus during the first trimester of pregnancy, causing fetal drug accumulation **(4, 44).**

The use of precise histopathological studies to investigate the pathogenesis of placental toxicity is thought to be a useful tool for understanding the mechanism of teratogenicity and developmental toxicity with embryo mortality **(45).**

The results of this study confirmed that pregnant rats given therapeutic doses of DS, had severe structural deterioration of the placenta. The lesions of basal zone were in the form of massive cystic degeneration of glycogen cells and decreased number and necrosis of spongiotrophoblasts and trophoblastic giant cells. Similar placental degenerative changes were seen in previous literatures that used Diclofenac Potassium **(29).**

Furukawa et al. (45) stated that the emergence of widespread cytoplasmic vacuolation within glycogen cells, followed by cytolysis and amalgamation to form giant cysts filled with homogenous acidophilus material and cell debris, may explain the presence of enormous coalescing cysts that indicated massive cystic degenerations of glycogen cells in our current work.

On the other hand, The materno-embryonic gases exchange and nutrition is thought to take place in the labyrinth, according to previous investigation **(46).** In the current study, necrosis of trophoblastic cells, marked vasodilatation and congestion of maternal sinusoids and fetal capillaries, ruptured capillaries with extensive internal hemorrhage in the labyrinth zone were clearly seen in the treated placenta. Similar degenerative findings were also observed in other previous studies **(29, 43, 47). Furukawa et al. (45)** revealed that trophoblasts in the fetal part of the placenta have been discovered to be a common target for chemical and pharmacological toxicity due to their high proliferative activity. On the other hand, the trophoblastic Giant cells are assumed to be progenitor cells for highly differentiated trophoblasts, and their degeneration causes trophoblast reduction, according to these researchers **(48)**.

The necrosis in the labyrinth and in maternal decidua in the current study were also mentioned by **Omer et al. (43)** who attributed this finding due to poor maternal vascular circulation and low utero/placental/fetal oxygenation. According also to the study of **Price et al. (34),** who concluded that taking NAIDs during the third trimester of pregnancy can have negative consequences such as altering uteroplacental blood flow.

The vascular congestion, ruptured capillaries and extensive internal hemorrhage of the labyrinth zone in our results indicated the breakdown of placental blood barrier that separates the maternal blood from fetal capillaries and so allowing the maternal and fetal blood to mix. This finding was also mentioned before by **Hosseini et al. and Omer et al. (43, 47)** who claims that significant labyrinth congestion indicates a malfunction within the placental blood barrier, with consequent decrease of nutrients reaching the fetal circulation.

The liver is an essential organ for detoxification in the mammalian system that is essential for metabolic activities, waste disposal, and purification**.** Because the liver is the primary site for biotransformation and detoxification, it is exposed to a large number of harmful metabolites **(41).**

The current study revealed many signs of hepatic structure deteriorations in both neonatal and adult treated groups after maternal exposure to therapeutic dose of DS. The lesions in maternal liver were in the form of; dilatation and congestion of central veins and blood sinusoids, proliferation of kupffer lining cells, swelling, vacuolar degeneration and necrosis of hepatocytes, marked dilatation and congestion of portal vein, proliferation of bile ductules, thickening of wall of portal vein, hepatic arteries and connective tissue surrounding as well. Similar histopathological changes in adult liver also observed in the previous literatures **(29, 49).**

Although NSAIDs include a hepatotoxicity warning, diclofenac and sulindac appear to be the most usually linked to the condition **(50).** Moreover, acute diclofenac exposure for 7 days induced histological changes in the adult rat liver **(51, 52).**

In addition to the congestion and dilatation of the central vein**s** that observed in the neonatal treated liver in this work, extensive cytoplasmic vacuolations of hepatocytes, distorted epithelial lining of central vein and increased number of hematopoietic (blood forming) cells and binucleated giant cells were also clearly recorded.

Previous research has concluded that NSAIDs should not be used because of the known risk of fetotoxicity. NSAIDs can cause a premature closure of fetal ductus arteriosus (DA) that leads to respiratory problems, pulmonary hypertension, and unwanted impacts on kidney function; this results in oligohydramnios and neonatal anuria **(13-15, 53)**. With increasing gestational age, the risk of ductal constriction and associated problems increases. In the late third trimester, the ductus arteriosus is extremely sensitive to prostaglandin inhibitors **(54).**

The most prominent consequence of DS could be due to the constriction of the DA caused by DS, which results in a reduction in the amount of oxygen-poor blood reaching the liver tissue and possibly liver parenchymal cell deterioration. As a result of the restricted DA, pulmonary vascular resistance can develop, leading to right ventricular dilation and tricuspid insufficiency. Insufficiency of the right ventricle impacts the liver, causing hyperemia and/or congestion as a result of stasis. The inadequate oxygenation of the liver causes dilated sinusoids, degenerated hepatocytes and even death of parenchymal cells **(55).**

On the hand, Diclofenac is reported to alter the normal physiological metabolic activities of liver and was implicated to hepatotoxicity due to the production of reactive metabolites and reactive oxygen species (ROS). Reactive metabolites of diclofenac, such as DAG, 4′-and 5-hydroxydiclofenac, and 2,5-quinone imines, contribute to the severity of toxicity **(56),** by creating covalent modification of proteins that conjugate with glutathione to form glutathione (GSH) adducts, provoking immunological responses against these protein adducts and alteration of cellular proteins **(57).** The significance of these protein adducts in the pathogenesis of DCF-related liver damage, however, is unknown **(58).**

Regarding the DS effects on the fetal lung in this work, the lung tissue showed features of acute pulmonary inflammation in the form of shrinkage of lung tissue, marked reduction of air spaces, extensive cytoplasmic vacuolations in mesenchymal cells of lung parenchyma and within the epithelium of terminal bronchioles, edema and hemorrhage of mesenchyme, dispersed blood spots between the mesenchymal tissues and congestion of pulmonary blood vessels. As demonstrated by **(59)** that acute lung injury (ALI) and acute respiratory distress syndrome (ARDS) are disorders characterized by inflammation, deterioration of lung function, and increased vascular permeability. It is the lung's reaction to viral, inflammatory, and chemical insults, as well as trauma. A major feature of ALI/ARDS is the disruption of the blood-air barrier, which is followed by inflammatory cell influx and edema development.

Xenobiotic metabolism in the lung, an organ of initial entry for xenobiotics into the body, is critical for inhaled substances entering this organ both voluntarily (e.g. drugs) and accidentally (e.g. pollutants). Furthermore, local metabolism by enzymes that predominantly or mainly occur in the lungs is critical for the beneficial or harmful effects of xenobiotics that enter the body by pathways other than breathing **(60).**

In the current study we chose intraperitoneal injection as the drug's route of administration to avoid the drug's hepatic first-pass metabolism before it entered the systemic circulation. This is in accordance with **Yilmaz et al. (38)** who stated that lungs are a well-perfused organ that receives the whole cardiac output. Consequently, all drugs given intravenously, intramuscularly, subcutaneously, or topically pass through the lungs before reaching the liver. Because circulating molecules will be exposed to pulmonary enzymes, pulmonary first pass may be important for drugs given through these routes and this may explain in this study why statistically, the most affected organ in neonates was the lung if compared with other treated organs.

The fetal toxicity was explained by prostaglandin suppression by NSAIDs, as prostaglandins produced in various tissues and membranes played a critical role in embryonic development **(61)**. Therefore, prostaglandins (PGE2) plays significant roles in the lung and supports lung microvascular integrity. Therefore, PGE2 could be the epithelium-derived, barrier-promoting mediator **(62).** Prostaglandins (PGE2) are metabolites of arachidonic acid that act by binding to four distinct G protein coupled receptors (EP1-EP4) with tissue-specific distribution. It enhances the barrier function of human and mouse pulmonary microvascular endothelial cells via EP4 receptor activation and diminished the barrier disruption induced by lipopolysaccharide (LPS)-induced acute lung injury **(63).** Furthermore, under basic conditions, primary mouse alveolar epithelial cells type I (ATI) cells released large levels of PGE2. Release of PGE2 was noticeably diminished by Diclofenac administration **(59).**

Additionally, the most prominent features of histopathological examination of lung tissue in the current study were hemorrhage, congestion and edema which are in accordance with and can be explained by **Siu and Lee (15)** who found that early closure of the DA after short-term maternal exposure to DS caused severe pulmonary hypertension and transient hypertrophic cardiomyopathy on the right side of the heart in neonatal rats.

On contrast to the results of current study, there was no apparent change in lung histological examination between the control and DS-treated prenatal groups in previous study **(36)**. This discrepancy could be due to the various measures used in the DS -treated group, which the drug was

given by IP injection between days 5 and 19 gestational age of pregnancy. While the time of sacrifice was at postnatal weeks 4 and 20 (12 pups). Consequently the prolonged discontinuation of the drug can cause recovery as demonstrated by **Ueda et al. (64)** who hypothesized that DS-induced pneumonitis would resolve quickly if the diclofenac was stopped.

According to neonatal cardiomyocytes of the ventricular wall treated with DS, the histopathological results in the current study revealed massive degenerative changes including extensive cytoplasmic vacuolations and nuclear pyknosis of cardiomyocytes with extracellular edema in between. These results were in agreement with **Gevrek et al. (5)** as they reported more extracellular matrix and weaker muscle fibers. **Ghosh et al. (65)** also suggested that pharmacological levels of diclofenac in diclofenac treated heart mice caused cardiac cell death in neonatal cardiomyocytes with cardiac dysfunction.

The results suggested that diclofenac may exert its effect on cardiac cells was by inhibiting mitochondrial C-III activity which leads to excessive ROS generation (65). Moreover, it could prevent several mechanisms, such as phospholipase C enzyme activation, ion transport, mitochondrial oxidative phosphorylation, and cell interaction **(66).**

The marked congestion of blood vessels and extravasated hemorrhage which have reported in neonatal heart in our results, can be explained by previous studies reported that DS has some important, specific, and adverse effects on the ductus arteriosus (DA), the most important being the contraction of the fetal DA **(67).** Narrowing or closure of fetal DA was described in 33 human fetuses in the 2nd trimester **(40)**. The most prominent effect contraction of the fetal DA may result in negative events such as escape back to the tricuspid encountering marked congestion of blood vessels and rupture of blood capillaries revealing the presence of the extensive areas of hemorrhage, right sided ventricular heart failure, and shunting between the atriums in the heart.

From the previous discussion, our results concluded that, by prenatal administration of therapeutic dose of DS, there were significant histopathological changes in all DS-treated groups of both mothers and their neonates.

Moreover, in the current study, the statistical results showed highly significant increase in the mean values of area percentages of positive TNF-α and iNOS immuno-reactions (**P** <0.0001) within the DS-treated groups when compared to their control groups in all studied groups.

Among the three types of NSAIDs, diclofenac is regarded to be the most potent non-selective COX inhibitor among NSAIDs, capable of increasing expression of the key proinflammatory cytokine; tumor necrosis factor-α (TNF-α). As a result, the degree of COX inhibition is correlated with rising of TNF-α levels **(24, 68, 69)** and so may worsen the proinflammatory environment both inside the rheumatoid arthritis joint and across the body **(70)**. In addition, TNF-α is the key factor in the pathogenesis of indomethacin-induced small intestinal damage and it may be a potential target for treating NSAID-induced small intestine injury **(71).**

Furthermore, TNF-α stimulates the activation of NF-κB in the epithelial cells with the production of different inflammatory chemokines consequently, recruitment of the different immune cells initiating an inflammatory response **(72).**

On the other hand, the iNOS generates enormous amounts of a free radical gas known as nitric oxide (NO). upon stimulation by excess proinflammatory cytokines e.g. TNF-α and Interferon gamma. In pathological circumstances, iNOS is considered a detrimental enzyme and is thought to be a key contributor to cardiovascular disorders such as atherosclerosis **(73, 74).** Induction of the high-output iNOS usually occurs in an oxidative environment, and thus large amounts of NO have the chance to react with superoxide O_2^- (precursor of most reactive oxygen species (ROS), leading to peroxynitrite production and cell toxicity **(75).** Moreover, NO is a potent smooth relaxant, which can be produced from iNOS by the induction of TNF-α **(76).**

From our finding result and from previous literatures, the oxidative stress in addition to TNF-α release are the key mechanisms of DS-induced organ harm in both maternal and neonatal organs.

CONCLUSION

The current investigation found that giving therapeutic doses of DS during the period of organogenesis caused significant histopathological alterations in both maternal and newborn organs, as well as enhancing the inflammatory response by up-regulation of pro-inflammatory markers linked to oxidative stress.

Author contributions:

All authors made equal contributions to this study.

Funding:

This study was not funded by any source.

Conflicts of Interest

No potential conflict of interest relevant to this article was reported.

REFERENCES

1. Adeyemi WJ, Omoniyi JA, Olayiwola A, Ibrahim M, Ogunyemi O, Olayaki LA. Elevated reproductive toxicity effects of diclofenac after withdrawal: Investigation of the therapeutic role of melatonin. Toxicol Rep., 2019;6:571-7.
2. Pangtey GS, Agarwal N. Nonsteroidal Anti-inflammatory Drug Use During Pregnancy and Lactation: Effects on Mother and Child. Women's Health in Autoimmune Diseases: Springer; 2020. p. 215-9.
3. Smith SR, Deshpande BR, Collins JE, Katz JN, Losina E. Comparative pain reduction of oral non-steroidal

anti-inflammatory drugs and opioids for knee osteoarthritis: systematic analytic review. Osteoarthritis Cartilage., 2016;24(6):962-72.
4. Antonucci R, Zaffanello M, Puxeddu E, Porcella A, Cuzzolin L, Dolores Pilloni M, et al. Use of non-steroidal anti-inflammatory drugs in pregnancy: impact on the fetus and newborn. Curr Drug Metab., 2012;13(4):474-90.
5. Gevrek F, Kara M, RAĞBETLİ MÇ, ASLAN H. Effects of prenatally exposed diclofenac sodium on rat heart tissue: a stereological and histological study. Turk J Med Sci., 2015;45(3):474-80.
6. Werler MM, Mitchell AA, Hernandez-Diaz S, Honein MA. Use of over-the-counter medications during pregnancy. Am J Obstet Gynecol., 2005;193(3):771-7.
7. Li D, Ferber J, Odouli R, Quesenberry C. Use of Nonsteroidal Antiinflammatory Drugs During Pregnancy and the Risk of Miscarriage. Obstet. Anesth. Dig., 2019;39(2):93-4.
8. Nielsen GL, Sorensen HT, Larsen H, Pedersen L. Risk of adverse birth outcome and miscarriage in pregnant users of non-steroidal anti-inflammatory drugs: population based observational study and case-control study. Bmj. website, https://www.bmj.com/content/322/7281/266.short, 2001;322(7281):266-70.
9. Abd El-Rhaman HA, Mohamed ZA-H, Sultan ARS, Tawfik A-R. Assessment of the Effect of Non-steroidal Anti-inflammatory Drug (Diclofenac Potassium) on the Pregnant Rats and their Fetuses. Int. J. Pharm. Sci. Rev. Res., 58(2), September - October 2019; Article No. 08, Pages: 45-53.
10. Chae J-P, Park MS, Hwang Y-S, Min B-H, Kim S-H, Lee H-S, et al. Evaluation of developmental toxicity and teratogenicity of diclofenac using Xenopus embryos. Chemosphere., 2015;120:52-8.
11. Scherneck S, Schöpa FL, Entezami M, Kayser A, Weber-Schoendorfer C, Schaefer C. Reversible oligohydramnios in the second trimester of pregnancy in two patients with long-term diclofenac exposure. Reprod Toxicol., 2015;58:61-4.
12. Källén BA, Olausson PO. Maternal drug use in early pregnancy and infant cardiovascular defect. Reprod Toxicol.,. 2003;17(3):255-61.
13. Auer M, Brezinka C, Eller P, Luze K, Schweigmann U, Schwärzler P. Prenatal diagnosis of intrauterine premature closure of the ductus arteriosus following maternal diclofenac application. Ultrasound Obstet Gynecol., 2004;23(5):513-6.
14. Mersal A, Attili I, Alkhotani A. Severe neonatal pulmonary hypertension secondary to antenatal maternal diclofenac ingestion reversed by inhaled nitric oxide and oral sildenafil. Ann Saudi Med., 2007;27(6):448-9.
15. Siu K, Lee W. Maternal diclofenac sodium ingestion and severe neonatal pulmonary hypertension. J Paediatr Child Health., 2004;40(3):152-3.
16. Benini D, Fanos V, Cuzzolin L, Tatò L. In utero exposure to nonsteroidal anti-inflammatory drugs: neonatal renal failure. Pediatr Nephrol., 2004;19(2):232-4.
17. Chan L, Chiu P, Siu S, Lau T. A study of diclofenac-induced teratogenicity during organogenesis using a whole rat embryo culture model. Hum Reprod., 2001;16(11):2390-3.
18. Canan S, Aktaş A, Ulkay MB, Colakoglu S, Ragbetli MC, Ayyildiz M, et al. Prenatal exposure to a non-steroidal anti-inflammatory drug or saline solution impairs sciatic nerve morphology: a stereological and histological study. Int J Dev Neurosci., 2008;26(7):733-8.
19. Sriuttha P, Sirichanchuen B, Permsuwan U. Hepatotoxicity of nonsteroidal anti-inflammatory drugs: a systematic review of randomized controlled trials. Int J Hepatol., 2018;2018.
20. Björnsson ES. Hepatotoxicity by drugs: the most common implicated agents. Int J Mol Sci., 2016;17(2):224.
21. Gupta R. Pain management. Essential Topics for Examinations. eBook, Springer-Verlag Berlin Heidelberg. Springer is part of Springer Science+Business Media (www.springer.com) 2014. 45-8 p.
22. Aygün D, Kaplan S, Odaci E, Onger ME, Altunkaynak ME. Toxicity of non-steroidal anti-inflammatory drugs: a review of melatonin and diclofenac sodium association. Histol Histopathol., 2012;27(4):417-36.
23. Elibol E, KAPLAN S, Altun G, Aksoy A, Altunkaynak BZ. The effects of different doses of diclofenac sodium on newborn rat hippocampus exposed during the third trimester. Turk J Vet Ani Sci., 2020;44(2).
24. Mustafa HN, Alkan I, Deniz ÖG, Altunkaynak BZ, Annaç E, Kaplan S. A Study on the Toxic Effect of Different Doses of Diclofenac Sodium on the Development of the Kidney in the Postnatal Period. *Int. J. Morphol.*, 2019;37(3).
25. Sabry SA, Sakr SM, Shahin M, editors. Histological and Ultrastructural Studies on the Effect of Diclofenac Sodium on the Renal Cortex of Fetuses of Albino Mice. Glob J Pharm., 8 (3): 369-377, 2014.
26. Arslan H, Aktaş A, Elibol E, Esener OBB, Türkmen AP, Yurt KK, et al. Effects of prenatal diclofenac sodium exposure on newborn testis: a histomorphometric study. Biotech Histochem., 2016;91(4):277-82.
27. Ragbetli MC, Ozyurt B, Aslan H, Odaci E, Gokcimen A, Sahin B, et al. Effect of prenatal exposure to diclofenac sodium on Purkinje cell numbers in rat cerebellum: a stereological study. Brain Res., 2007;1174:130-5.
28. Güven D, Altunkaynak BZ, Ayranci E, Kaplan S, Bildircin FD, Kesim Y, et al. Stereological and histopathological evaluation of ovary and uterine horns of female rats prenatally exposed to diclofenac sodium. J Obstet Gynaecol., 2013;33(3):258-63.
29. Tawfik A-R, Alduweesh N, Mohamed Z, Sultan A, El-Rahman H. The histopathological effect of diclofenac potassium on maternal and fetal tissues. Int J Res Pharm Sci., 2020;11:2866-78.
30. EMEA. The European Agency for the Evaluation of Medicinal Products, Veterinary, Medicines and Inspections. Committee for Veterinary Medicinal Products –Diclofenac. . Report EMEA/MRL/03-FINAL, EMEA, 2003 https://wwwemaeuropaeu/en/documents/mrl-report/diclofenac-summary-report-committee-veterinarymedicinal-products_enpdf. 2003.
31. IACUC. Non-pharmaceutical and Pharmaceutical Grade Compounds in Research Animals. . Institutional

Animal Care and Use Committee, Office of Research Compliance (ORC) https://researchiuedu/doc/compliance/animal-care/bloomington/iub-biacuc-non-pharmaceutical-andpharmaceutical-gradecompounds-in-researchanimalspdf. 2013.
32. Bancroft JD, Layton C. The hematoxylins and eosin. In: Suvarna, KS, Layton, C, Bancroft, JD (ed) Bancroft's theory and practice of histological techniques E-Book. Ch:10, Pp 126-138. . 8th ed. ed: Elsevier Health Sciences; 2018. p.
33. Al Drees A, Khalil MS, Soliman M. Histological and immunohistochemical basis of the effect of aminoguanidine on renal changes associated with hemorrhagic shock in a rat model. Acta Histochem Cytochem., 2017:16025.
34. Price HR, Lai D, Kim H, Wright TE, Coughtrie MW, Collier AC. Detection and quantitation of non-steroidal anti-inflammatory drug use close to the time of birth using umbilical cord tissue. Toxicol Rep., 2020;7:1311-8.
35. US.FDA USFaDA. FDA Drug Safety Communication: FDA has reviewed possible risks of pain medicine use during pregnancy. Available at: https://wwwfdagov/drugs/drug-safety-and-availability/fda-drug-safety communication-fda-hasreviewed-possible-risks-pain-medicine-useduring-pregnancy 2016; Accessed August 25,2020.
36. Ragbetli C, Ilhan F, Aydinlioğlu A, Kara M, Ragbetli MC. A histological investigation concerning the effects of diclofenac sodium to the lung in 4- and 20-week-old rats treated prenatally. J Matern Fetal Neonatal Med., 2011;24(2):208-12.
37. Cappon GD, Fleeman TL, Cook JC, Hurtt ME. Combined treatment potentiates the developmental toxicity of ibuprofen and acetazolamide in rats. Drug Chem Toxicol.,, 2005;28(4):409-21.
38. Yilmaz Y, Williams G, Walles M, Manevski N, Krähenbühl S, Camenisch G. Comparison of rat and human pulmonary metabolism using precision-cut lung slices (PCLS). Drug Metab Lett., 2019;13(1):53-63.
39. Christian MS, Goeke JE. handbook of developmental toxicology in Hood ,RD(ed)p:529,Boca Raton:CRC press. 1997.
40. Dathe K, Hultzsch S, Pritchard LW, Schaefer C. Risk estimation of fetal adverse effects after short-term second trimester exposure to non-steroidal anti-inflammatory drugs: a literature review. Eur J Clin Pharmacol., 2019;75(10):1347-53.
41. Sathishkumar P, Mohan K, Meena RAA, Balasubramanian M, Chitra L, Ganesan AR, et al. Hazardous impact of diclofenac on mammalian system: Mitigation strategy through green remediation approach. J Hazard Mater., 2021;419:126135.
42. Griffiths SK, Campbell JP. Placental structure, function and drug transfer. BJA Educ., 2015;15(2):84-9.
43. Omer H, Kutb M, Kaatabi H. Histopathological changes in placenta of rat induced by levtricetam. Int J Neurorehabil., 2014;1(134):2376-0281.1000134.
44. Siu S, Yeung J, Lau T. A study on placental transfer of diclofenac in first trimester of human pregnancy. Hum Reprod., 2000;15(11):2423-5.
45. Furukawa S, Hayashi S, Usuda K, Abe M, Hagio S, Ogawa I. Toxicological pathology in the rat placenta. J Toxicol Pathol., 2011;24(2):95-111.
46. Syme M, Paxton JW, Keelan JA. Drug transfer and metabolism by the human placenta. Clin Pharmacokinet., 2004;43(8):487-514.
47. Hosseini E, Monfared AL, Moloudizargari M, Aghajanshakeri S, Toloomoghaddam S, Rahmatigavari S, et al. Histological and morphological characteristics of placenta in the rats administrated with Glycyrrhiza glabra extract. Res Opin Anim Vet Sci., 2013;3(2):60-3.
48. Kosif R, Öztekin A. Microscopic examination of placenta of rats prenatally exposed to Aloe barbadensis: A preliminary study. Int. J. Morphol., 26(2):275-281, 2008.
49. Aydin G, Gökçimen A, Öncü M, Çicek E, Karahan N, Gökalp O. Histopathologic changes in liver and renal tissues induced by different doses of diclofenac sodium in rats. Turk J Vet Anim Sci., 2003;27(5):1131-40.
50. O'connor N, Dargan PI, Jones AL. Hepatocellular damage from non-steroidal anti-inflammatory drugs. Q J Med., *An International Journal of Medicine*, 96(11):787–791 2003, https://doi.org/10.1093/qjmed/hcg138 Downloaded from https://academic.oup.com/qjmed/article/96/11/787/1586888 by guest on 02 October 2021
51. Al-Dossari MH, Fadda LM, Attia HA, Hasan IH, Mahmoud AM. Curcumin and selenium prevent lipopolysaccharide/diclofenac-induced liver injury by suppressing inflammation and oxidative stress. Biol Trace Elem Res., 2020;196(1):173-83.
52. Riane K, Sifour M, Ouled-Haddar H, Espinosa C, Esteban MA, Lahouel M. Effect of probiotic supplementation on oxidative stress markers in rats with diclofenac-induced hepatotoxicity. Braz. J. Microbiol., 2020:1-8.
53. Gewillig M, Brown SC, De Catte L, Debeer A, Eyskens B, Cossey V, et al. Premature foetal closure of the arterial duct: clinical presentations and outcome. Eur Heart J., 2009;30(12):1530-6.
54. Moise Jr KJ. Effect of advancing gestational age on the frequency of fetal ductal constriction in association with maternal indomethacin use. Am J Obstet Gynecol. 1993;168(5):1350-3.
55. Gökçimen A, Aydin G, Karaöz E, Malas MA, Öncü M. Effect of Diclofenac Sodium Administration during Pregnancy in the Postnatal Period. Fetal Diagn Ther., 2001;16(6):417-22.
56. Kawase A, Hashimoto R, Shibata M, Shimada H, Iwaki M. Involvement of reactive metabolites of diclofenac in cytotoxicity in sandwich-cultured rat hepatocytes. Int J Toxicol., 2017;36(3):260-7.
57. Tang W. The metabolism of diclofenac-enzymology and toxicology perspectives. Curr Drug Metab., 2003;4(4):319-29.
58. Aithal GP, Day CP. Nonsteroidal anti-inflammatory drug–induced hepatotoxicity. Clin Liver Dis., 2007;11(3):563-75.
59. Bärnthaler T, Maric J, Platzer W, Konya V, Theiler A, Hasenöhrl C, et al. The role of PGE 2 in alveolar epithelial and lung microvascular endothelial crosstalk. Sci Rep., 2017;7(1):1-17.
60. Oesch F, Fabian E, Landsiedel R. Xenobiotica-metabolizing enzymes in the lung of experimental animals, man and in human lung models. Arch Toxicol., 2019;93(12):3419-89.

61. Fortier M, Krishnaswamy K, Danyod G, Boucher-Kovalik S, Chapdalaine P. A postgenomic integrated view of prostaglandins in reproduction: implications for other body systems. J Physiol Pharmacol., 2008;59(Suppl 1):65-89.
62. Cheng S-E, Lee I-T, Lin C-C, Wu W-L, Hsiao L-D, Yang C-M. ATP mediates NADPH oxidase/ROS generation and COX-2/PGE2 expression in A549 cells: role of P2 receptor-dependent STAT3 activation. PloS one., 2013;8(1):e54125.
63. Konya V, Maric J, Jandl K, Luschnig P, Aringer I, Lanz I, et al. Activation of EP 4 receptors prevents endotoxin-induced neutrophil infiltration into the airways and enhances microvascular barrier function. Br J Pharmacol. 2015;172(18):4454-68.
64. Ueda K, Sakano H, Tanaka T, Hayashi M, Fujita N, Zempo N. Diclofenac (voltaren)-induced pneumonitis after chest operation. Ann Thorac Surg., 2002;74(6):2176-7.
65. Ghosh R, Goswami SK, Feitoza LFB, Hammock B, Gomes AV. Diclofenac induces proteasome and mitochondrial dysfunction in murine cardiomyocytes and hearts. Int J Cardiol., 2016;223:923-35.
66. Aygün D, Kaplan S, Odaci E, Onger ME, Altunkaynak ME. Toxicity of non-steroidal anti-inflammatory drugs: a review of melatonin and diclofenac sodium association. Histol Histopathol., 2012; 27: 417-436. DOI: 10.14670/HH-27.417.
67. Dos Santos CS, Silva PV, Castelo R, Tiago J. Premature closure of ductus arteriosus after a single dose of diclofenac during pregnancy. BMJ Case Reports CP., 2021;14(6):e243485.
68. Çağıltay E, Kaplan M, Nalbant S, Akpak YK, Sahan B, Akmaz İ. Does non-steroidal anti-inflammatory drugs increase tumor necrosis factor-alpha levels? Int J Res Med Sci., 2015 Sep;3(9):2280-2283 www.msjonline.org.
69. Nouri A, Heidarian E, Nikoukar M. Effects of N-acetyl cysteine on oxidative stress and TNF-α gene expression in diclofenac-induced hepatotoxicity in rats. Toxicol Mech Methods., 2017;27(8):561-7.
70. Page TH, Turner JJO, Brown AC, Timms EM, Inglis JJ, Brennan FM, et al. Nonsteroidal Anti-Inflammatory Drugs Increase TNF Production in Rheumatoid Synovial Membrane Cultures and Whole Blood. J Immunol., 2010; 185(6):3694-3701; http://www.jimmunol.org/content/185/6/3694, doi: 10.4049/jimmunol.1000906.
71. Fukumoto K, Naito Y, Takagi T, Yamada S, Horie R, Inoue K, et al. Role of tumor necrosis factor-α in the pathogenesis of indomethacin-induced small intestinal injury in mice. Int J Mol Med., 2011;27(3):353-9.
72. Ruder B, Atreya R, Becker C. Tumour necrosis factor alpha in intestinal homeostasis and gut related diseases. Int J Mol Sci., 2019;20(8):1887.
73. Lind M, Hayes A, Caprnda M, Petrovic D, Rodrigo L, Kruzliak P, et al. Inducible nitric oxide synthase: good or bad? Biomedicine & Pharmacotherapy., 2017;93(9):370-375. DOI: 10.1016/j.biopha.2017.06.036
74. Sudar E, Dobutovic B, Soskic S, Mandusic V, Zakula Z, Misirkic M, et al. Regulation of inducible nitric oxide synthase activity/expression in rat hearts from ghrelin-treated rats. J Physiol Biochem., 2011;67(2):195-204.
75. Mungrue IN, Husain M, Stewart DJ. The role of NOS in heart failure: lessons from murine genetic models. Book title:The Role of Nitric Oxide in Heart Failure. 2004:113-128.
76. Li A, Xiong J, Chen Z. IL-6, TNF-α, and iNOS is associated with decreased colonic contraction in rats with multiple organ dysfunction syndrome. J Surg Res., 2012;178(2):e51-e7.

How to cite

Mokhtar, H., Alabassery, N., Sabry, R. Histological and Immunohistochemical Study on the Effect of Prenatal Administration of Diclofenac Sodium on Maternal and Neonatal Organs in albino rat. Zagazig University Medical Journal, 2023; (566-582): -. doi: 10.21608/zumj.2021.97027.2352